NASA TECHNICAL NOTE

NASA TN D-4829

NASA TN D-4829

LOW-DENSITY, LEADING-EDGE BLUNTNESS, AND ABLATION EFFECTS ON WEDGE-INDUCED LAMINAR-BOUNDARY-LAYER SEPARATION AT MODERATE ENTHALPIES IN HYPERSONIC FLOW

by C. L. W. Edwards and John B. Anders

Langley Research Center
Langley Station, Hampton, Va.

NATIONAL AERONAUTICS AND SPACE ADMINISTRATION • WASHINGTON, D. C. • OCTOBER 1968

LOW-DENSITY, LEADING-EDGE BLUNTNESS, AND ABLATION EFFECTS ON WEDGE-INDUCED LAMINAR-BOUNDARY-LAYER SEPARATION AT MODERATE ENTHALPIES IN HYPERSONIC FLOW

By C. L. W. Edwards and John B. Anders

Langley Research Center
Langley Station, Hampton, Va.

NATIONAL AERONAUTICS AND SPACE ADMINISTRATION

For sale by the Clearinghouse for Federal Scientific and Technical Information
Springfield, Virginia 22151 – CFSTI price $3.00

LOW-DENSITY, LEADING-EDGE BLUNTNESS, AND ABLATION EFFECTS ON WEDGE-INDUCED LAMINAR-BOUNDARY-LAYER SEPARATION AT MODERATE ENTHALPIES IN HYPERSONIC FLOW

By C. L. W. Edwards and John B. Anders
Langley Research Center

SUMMARY

A study of real-gas wedge-induced laminar-boundary-layer separation has been made. The investigation was conducted in low-density air on a highly cooled flat-plate model with interchangeable leading edges and various trailing-edge flap angles. All tests were conducted in the Langley 1-foot hypersonic arc tunnel at a nominal free-stream Mach number of 12, free-stream unit Reynolds numbers from 1.1×10^4 to 2.7×10^4 per foot $\left(3.6 \times 10^4 \text{ to } 8.9 \times 10^4 \text{ per meter}\right)$, and dimensionless stagnation enthalpies from 39.0 to 72.4. The extent of separation was found to increase with increasing leading-edge bluntness at these test conditions. Significant low-density effects are shown to delay the onset of separation in comparison with what would be expected from predictions by a strong-interaction theory. The direct effect of mass addition on the extent of separation through ablative leading edges was found to be negligible; however, an indirect effect on the extent of separation due to leading-edge regression was found to be significant.

INTRODUCTION

The continued interest in maneuverable entry vehicles has focused renewed attention on boundary-layer separation. Conventional controls utilizing deflected surfaces may create the problem of boundary-layer separation directly ahead of the controls. Hypersonic flight of the vehicles further complicates the problem because the thickened boundary layers require greater deflections of larger control surfaces than those previously required for supersonic flight. The result could be more extensive boundary-layer separation at hypersonic speeds than that encountered at supersonic speeds. Also, the increase in kinetic energy associated with hypersonic flight now requires a vehicle designer to consider thermodynamic imperfections in the flow field and the protection of the vehicle from the high heating rates encountered. One method of heat protection is ablation cooling. However, the ablation products enter the flow field adjacent to the vehicle and may possibly influence its aerodynamic characteristics and the behavior of any flow separation.

Up to this time, all theoretical methods for laminar boundary layers and all experimental investigations with the exception of references 1, 2, and 3 have considered the fluid to be a perfect gas. Although there are several analyses for boundary-layer separation of a perfect gas (refs. 4 to 17), the additional complexities of a real gas do not readily lend themselves to solution. There are also limitations on the validity of these solutions as increasing rarefaction effects are encountered at very low Reynolds numbers; furthermore, the additional complexities of gas chemistry and mass addition are not fully understood. Consequently, it is not feasible at the present time to attempt to develop a theory which could account for the effects of real-gas chemistry, low Reynolds number, and mass injection on boundary-layer separation. However, a maneuverable entry vehicle may experience these effects during some phase of its flight trajectory and the arc-jet facilities now offer the opportunity to study some of the problem areas experimentally. The present investigation was initiated in such a facility to determine any gross trends that might appear in the three areas mentioned. Even though the low-density and real-gas effects cannot be individually isolated in this facility, an attempt is made to examine systematically some of the individual effects through model geometry variation.

SYMBOLS

A_1, A_2 constants in equation (1)

$c_{f,o}$ local skin-friction coefficient at beginning of interaction

$C_{p,p}$ plateau-pressure coefficient

$C_\infty = \dfrac{\mu_w T_\infty}{\mu_\infty T_w}$

d model nose diameter

h step height above plate

H_t tunnel stagnation enthalpy

L model length from leading edge to hinge line

L' length of wing chord, measured from leading-edge junction to hinge line (2.0 in. (5.08 cm))

$\dot{m}$ mass-flow rate

$\dot{m}_{BL}$	boundary-layer mass-flow rate
M_o	Mach number at beginning of interaction
M_∞	free-stream Mach number
p_{ref}	pressure at standard conditions $\left(1 \text{ atmosphere } \left(1.013 \times 10^5 \text{ N/m}^2\right)\right)$
p_t	stagnation pressure
$p_{t,2}$	pitot pressure in test section
p_w	pressure at wall
p_∞	free-stream pressure
R	gas constant
$R_{o,x}$	local Reynolds number at beginning of interaction, $\frac{\rho_o V_o x_o}{\mu_o}$
R_∞	free-stream unit Reynolds number
$R_{\infty,x}$	free-stream Reynolds number based on longitudinal distance
s	surface distance measured from wing-leading-edge junction (see fig. 2)
t	time
T_{ref}	temperature at standard conditions $\left(491.69^\circ \text{ R } \left(273.16^\circ \text{ K}\right)\right)$
T_t	stagnation temperature
T_w	wall temperature
T_∞	free-stream temperature
V_o	velocity at beginning of interaction
x	longitudinal coordinate

x_o longitudinal distance at beginning of interaction

x_s longitudinal distance to separation point

$\beta_o = \sqrt{M_o^2 - 1}$

θ ramp (flap or wedge) deflection angle

λ_∞ mean free path

μ_o coefficient of viscosity at beginning of interaction

μ_w coefficient of viscosity at wall

μ_∞ free-stream coefficient of viscosity

ρ_o mass density of air at beginning of interaction

τ leading-edge thickness (bluntness parameter)

$\bar{\chi}_{\infty,x}$ strong-interaction parameter, $M_\infty^3 \sqrt{C_\infty / R_{\infty,x}}$

APPARATUS AND TESTS

Test Facility

The present series of tests were conducted in the Langley 1-foot hypersonic arc tunnel. The test medium in this facility is electric-arc-heated air which is expanded in a 5^o half-angle conical nozzle to a nominal Mach number of 12. The inviscid core is approximately 5 inches (12.7 cm) in diameter. The test section Mach number gradient is approximately 0.03 per inch (0.0118 per cm). The test duration is up to 15 minutes. (A detailed description of the facility is presented in ref. 18.)

Models

The model used in the present study was an internally water-cooled flat plate spanning the test section and consisting of three basic parts: (1) interchangeable leading edges, (2) flat-plate wing, and (3) variable-angle trailing-edge flap (ramp). A schematic drawing of the model and pertinent dimensions are presented in figure 1.

Three types of leading edges were utilized: (a) sharp and water-cooled, (b) flat-face blunt and water-cooled, and (c) hemicylindrically blunted and ablative; these leading edges will be referred to herein as (a), (b), and (c), respectively. The ablative leading edges (c) were constructed of graphite, equal parts by weight of phenolic resin and powdered nylon (50-50 phenolic nylon), or teflon.

The internally water-cooled trailing-edge flap (ramp) had an angle range up to 45° (although tunnel blockage prevented testing beyond 35.5°). In addition to the variable flap, three forward-facing steps were employed in several auxiliary tests. The steps were uncooled and had heights above the plate of 0.250, 0.375, and 0.500 inch (0.635, 0.953, and 1.270 cm, respectively).

The complete model was fitted with two detachable end plates. The first set (see top sketch in fig. 1) was for leading edges (a) and (b), and the second set (see bottom sketch in fig. 1) was for leading edge (c).

Instrumentation

The model was instrumented with chromel-alumel thermocouples and 0.040-inch (0.102-cm) diameter pressure orifices. All pressure leads were of 0.060-inch (0.152-cm) inside diameter tubing in the model and were jumped to 0.090-inch (0.229-cm) inside diameter tubing immediately outside the model to reduce pressure lag as much as possible. The pressure leads were connected to ionization-type pressure sensors, and both the thermocouple and ionization gage outputs were monitored continuously on oscillograph film recorders. The model planform showing pertinent dimensions and the locations of pressure orifices and thermocouples is presented in figure 2.

Test Conditions and Data Accuracy

The present series of tests were conducted in air for free-stream Mach number M_∞ from 10.8 to 13.9, for dimensionless stagnation enthalpies H_t/RT_{ref} from 39.0 to 72.4, for free-stream unit Reynolds number R_∞ from 1.1×10^4 to 2.7×10^4 per foot $\left(3.6 \times 10^4 \text{ to } 8.9 \times 10^4 \text{ per meter}\right)$, and flap angles up to 35.5°. Tunnel blockage prevented flap angles greater than 36°. The ratio of wall temperature to stagnation temperature $\left(T_w/T_t\right)$ for the model was approximately 0.1. A list of individual test conditions is presented in table 1.

The maximum error in determining enthalpy for this facility is about ±8 percent (refs. 19 and 20). An orifice effect on pressure measurement for the conditions of these tests has been investigated and reported in reference 21. This effect can cause a maximum error in pressure measurements of -6 percent in the lowest pressures on the plate. The lowest pressures generally occur just prior to interaction. Maximum deviation due to the orifice effect on other pressures, such as those at separation, plateau, or reattachment, is considerably less than -6 percent. A maximum inaccuracy in instrumentation

and reading of data has been found to be 5 percent and -11 percent. The -11 percent includes the -6 percent maximum orifice effect mentioned above. The uncertainties in pressure cause an uncertainty in the calculation of local properties along the plate. A typical calculation was made by using the maximum uncertainty in pressure. This procedure was found to result in a 2-percent deviation in computed $c_{f,o}$ and a 4-percent deviation in local Mach number. The local flow properties on the sharp plate were determined by means of an oblique-shock compression from free-stream pressure to the measured pressure on the plate. The local flow properties over the blunted plates were determined by an isentropic expansion from measured pitot pressure to measured local pressures. Real-gas relations for equilibrium air were used in each instance.

THEORY

No general theory is available to assess completely the problem areas in boundary-layer separation resulting from a real gas, with very low Reynolds numbers, and from mass addition. However, there are some areas of study which might be considered individually, such as extent of separation and plateau pressures. The study of these areas as isolated problems neglects the basic problem, which is a description of the complete phenomenon of boundary-layer separation. These areas do have immediate importance, however, because a knowledge of the plateau-pressure level and the extent over which it acts is basic information that a designer would require. The important area of heat-transfer variation due to boundary-layer separation is not treated herein.

The technique used to assess the extent of separation is that presented in reference 3. This technique uses a simple oblique-shock representation of the boundary-layer separation phenomenon. It is restricted to free-interaction processes. Essentially, the technique involves calculating the plateau and reattachment pressure rises as functions of local conditions and then representing these pressure rises by oblique shocks. An iteration procedure is followed until the wedge angle required for the appropriate oblique-shock pressure rise just matches the physical angle of the ramp causing separation. This procedure is outlined in detail in reference 3, along with a sample calculation.

To date, there is no reliable simple method for determining plateau-pressure coefficient in laminar separated flow. The primary simple relation which is used to predict laminar plateau-pressure coefficient is

$$C_{p,p} = A_1\sqrt{\frac{c_{f,o}}{\beta_o}} = A_2\left(R_{o,x}\right)^{-1/4}\left(\beta_o\right)^{-1/2} \tag{1}$$

This expression was analytically derived in reference 15; the constants A_1 and A_2 were empirically determined primarily from the data of references 11 and 22. The value

of A_2 is taken as 1.82 (ref. 23) in this study. At best, the accuracy of this equation could be expected to be ±20 percent (ref. 24).

Low-density flows are not completely understood and are presently the object of considerable study; however, some low-density effects on boundary-layer separation should be predictable. Of course, one obvious result of lower density flows is the thickening of the boundary layer since displacement and momentum thicknesses are inversely proportional to Reynolds number (ref. 4). This increase in thicknesses requires larger flap deflections for the onset of separation, and increases separation and plateau-pressure coefficients. These effects are easily observed experimentally.

Another characteristic of low-density flows which can be considered is the possibility of slip flow at the wall. As rarefaction effects increase, the flow over a plate departs from that which is predicted by strong-interaction theory. Slip flow at the wall occurs and thereby changes the characteristics of the flow and the behavior of the separation region. The case of free molecule or transition flow has little or no direct application to boundary-layer separation because little or no boundary layer is actually developed in the regions. These regions are usually confined to a very small area near the leading edge and their effect on the overall characteristics of the flow is neglected in this study. The merged layer is a region characterized by a boundary layer from the plate surface to the shock (no inviscid region), a definite shock boundary (although possibly greatly thickened over that found in the strong-interaction area), and a wall-slip velocity which is less than the free-stream value This wall slip causes much fuller velocity profiles (ref. 25) than for the no-slip case. The increased momentum flux near the wall associated with these profiles should tend to delay separation. If a sufficient pressure gradient were present to cause separation in the merged-layer region, then the resulting extent of separation should be somewhat less than what would be expected from predictions by a strong-interaction theory. A good indicator of the onset of the merged-layer region is the rarefaction parameter $M_\infty\sqrt{C_\infty/R_{\infty,x}}$ (refs. 25 and 26). According to reference 25, the region $0.15 < M_\infty\sqrt{C_\infty/R_{\infty,x}} < 0.17$ is the boundary between strong interaction and the merged layer. All values of $M_\infty\sqrt{C_\infty/R_{\infty,x}}$ above 0.17 experience some slip flow. This result agrees with previous estimates of the upstream limit of strong-interaction theory based on surface measurements (ref. 25).

Real-gas effects in the moderate enthalpy range $\left(43 < H_t/RT_{ref} < 61\right)$ of reference 3 were found to be small and were fairly predictable by present theoretical methods if real-gas relationships were used to determine flow properties. Since the present study was conducted at approximately the same enthalpy range as that of reference 3, it was assumed that the determination of the flow properties using real-gas equations would adequately account for any differences from perfect-gas theory. All calculations were made on the basis of equilibrium flow.

RESULTS AND DISCUSSION

Sharp Plate with Variable-Angle Flap

No detectable separation could be generated ahead of the flap (ramp) prior to the maximum deflection of 35.3° when the sharp leading edge (a) was employed. This can be seen from the pressure distributions shown in figure 3. A small plateau might be faired at the hinge line for the 35.3° test; however, only one point is displaced from the smooth unseparated trend. Of course the ideal method to assess the existence of a plateau would be to test sufficient flap angles above 35°. Unfortunately, tunnel blockage problems were encountered for flap angles slightly above 35°. Nevertheless, the data obtained are believed to be significant even though the onset of separation is not exactly determined because the results obtained were unexpected on the basis of previous boundary-layer-separation studies. For example, the same basic plate was used to obtain the data of reference 3 with the exception of leading-edge and end-plate geometry. In that study, moderate amounts of separation were obtained with lower flap angles ($\leq 30^{\circ}$) for a model with a hemicylindrically blunted leading edge at approximately the same range of tunnel conditions. Other investigators (see refs. 27 to 29) have previously shown that separation tends to decrease with increasing leading-edge bluntness whereas the opposite trend is exhibited in the present study. If, however, the present sharp-leading-edge data were obtained in a merged-layer region, the results might have been predictable.

Figure 4 shows the pressure deviation (data from refs. 30 to 34) from strong-interaction theory for the 0° flap test. A figure similar to figure 4 has been previously used to illustrate pressure trends in the merged-layer region (fig. 18 of ref. 34). The presence of significant rarefaction is indicated by the fact that the present data have the same trend as previous data obtained in the merged layer. An estimate of the extent of the merged layer on the present sharp plate can be determined from the rarefaction parameter $M_{\infty}\sqrt{C_{\infty}/R_{\infty,x}}$. Figure 5 is a plot of the rarefaction parameter as a function of the distance from the leading edge for the present sharp-leading-edge flat-plate tests. The shaded horizontal band represents the McCroskey (ref. 25) value, $0.15 < M_{\infty}\sqrt{C_{\infty}/R_{\infty,x}} < 0.17$, for the onset of the merged layer. A merged layer is predicted over the entire distance from the leading edge to the hinge line. In addition, McCroskey (ref. 25), Becker and Boylan (ref. 34), and Pan and Probstein (ref. 35) indicate that wall slip can extend into the strong-interaction region; thereby the onset of separation is delayed, based on the discussion presented in the previous section.

For the sharp-leading-edge flat-plate tests, the delay in separation that was noted over that obtained from the blunt-leading-edge tests of reference 3 was to be expected. A clarification note should be inserted at this point concerning the sharp leading edge. The merged-layer analyses referenced previously apply to a "theoretically sharp" value which

occurs when the leading-edge thickness is several times smaller than the mean free path of the flow approaching it. For the present study, the leading-edge thickness τ was approximately 0.001 inch (0.0025 cm) whereas the mean free path λ_∞ had an approximate range of 0.010 to 0.020 inch (0.025 to 0.051 cm). Also, the lower-surface wedge angle for the leading edge was approximately 27^o which, according to Becker and Boylan (ref. 34) is small enough to insure a "sharp" leading edge.

Sharp Plate With Steps

The basic flat plate was fitted with a series of three forward-facing steps in order to cause more abrupt adverse pressure gradients than could be obtained with the flap at the maximum flap deflection obtainable. These steps were uncooled and had step heights above the plate (h) of 0.250, 0.375, and 0.500 inch (0.635, 0.953, and 1.270 cm, respectively). The pressure distributions of these tests are shown in figure 6. Separation definitely occurred ahead of the sharp plate with the two larger steps and possibly occurred ahead of all three. When the plateau pressures obtained with the steps were compared with those predicted by equation (1), the agreement was only fair. Figure 7 shows the agreement between the available experimental values of laminar plateau pressures (refs. 3, 11, 22, 23, and 36 to 39) and those predicted by equation (1). The previously unpublished data of J. F. Wayne are shown here by permission from the Boeing Company. The solid line represents equation (1) when the constant A_2 has a value of 1.82. The dashed lines represent ±20-percent deviation from theory. The overall deviation is considerable; nevertheless, the present tests are within the limits of deviation of previous experiments. This fact does not mean that there are no appreciable effects of real gas and/or low density on plateau pressure, but rather that they are indeterminate within the framework of the presently accepted relation for plateau pressure. The calculation technique presented in reference 3 for the extent of separation does not apply to separation ahead of steps and in the absence of another applicable technique no assessment is made of the extent of separation shown for these data.

Since the pressure levels prior to interaction (ref. 3) were adequately predicted by the no-slip method of Bertram and Blackstock (ref. 40) on a hemicylindrically blunted plate and the pressure levels prior to interaction were shown to exhibit apparent rarefaction effects for the sharp leading edge of this study, a series of leading-edge-bluntness tests were conducted to study the trends under conditions between these two studies. Three additional flat-face bluntnesses (τ) of 0.031, 0.063, and 0.094 inch (0.0788, 0.160, and 0.239 cm, respectively) were employed. The pressure distributions for these tests are shown in figure 8. In addition to the cooled flat-face blunt-leading-edge pressure distributions, a pressure distribution from a hemicylindrically blunt graphite leading edge (test 15) in which no ablation occurred is also shown. This leading edge was uncooled, but its effect on downstream separation is assumed to be negligible and is used

here as the no-slip boundary. Some apparent separation is seen for each of the additional bluntness tests shown. However, with the exception of the graphite leading edge, all the pressures prior to interaction are lower than those that would be predicted by no-slip theory. This type of pressure distribution would indicate the possibility of rarefaction effects on the plate. However, these leading edges do not closely approximate the "theoretically sharp" value and the rarefaction indicator range, $0.15 < M_\infty\sqrt{C_\infty/R_{\infty,x}} < 0.17$, is not applicable to determine the extent over which these effects might be felt. From the data shown in figure 8, there appears to be a gradual decrease in rarefaction effects and an apparent increase in the extent of separation as leading-edge bluntness is increased.

When the calculation technique of reference 3 for the extent of separation was applied to these data, the agreement became increasingly better with increasing leading-edge bluntness. This improvement is shown in figure 9, where θ is the flap deflection angle, τ is the bluntness height of the leading edge, and L is the length of the plate from leading edge to hinge line. As the value of τ/L is increased, the agreement between experiment and theory is seen to approach an asymptotic value approximately 10 percent under the exact agreement value of 1.0. Why the asymptote does not appear to be 1.0 is not known; however, the shape of the curve illustrates the point to be made here. As leading-edge bluntness is decreased, the calculated value of θ required to maintain the experimental extent decreases and thereby implies that separation should occur at smaller flap angles with decreasing leading-edge bluntness. This trend is in agreement with other no-slip investigations (for example, see refs. 27 to 29). The experimental value of θ required to maintain a given extent of separation, however, increases as leading-edge bluntness is decreased. This increase indicates possible rarefied flow effects which, from figure 9, become appreciable under the present test conditions when $\tau/L \lessapprox 10^{-2}$.

The plateau pressure levels are not clearly defined for the variable-bluntness tests shown between the faired "boundary" curves of figure 8. When the average values were compared with equation (1), the deviation was still within previous experimental limits, as shown by the half-shaded circular symbols in figure 7.

Ablative Leading Edges

A limited study of leading-edge ablation effects on separation was also conducted. The investigation was made with the same basic model and a series of ablative leading edges constructed of graphite, 50-50 phenolic nylon, and teflon. These leading edges were hemicylindrically blunted and are shown in the bottom sketch of figure 1. The enthalpy generated in this study was insufficient to cause graphite ablation, and the data obtained with these leading edges are used primarily as comparison data for the 50-50 phenolic-nylon and teflon ablation results.

Phenolic nylon is a charring ablator. For these tests, even though significant mass is lost through ablation, the leading edge retains its aerodynamic shape fairly well with only slight leading-edge regression. Teflon on the other hand is a subliming ablator and a significant amount of mass loss is reflected in a proportionally significant leading-edge regression. Calculated average ratios of the mass-flow rate of the ablative leading edge to the mass-flow rate of the boundary layer $\left(\dot{m}/\dot{m}_{BL}\right)$ were approximately 0.11 for the 50-50 phenolic nylon and 0.14 for teflon. These ratios are used only to show that the mass-addition rate was roughly the same for both ablators, and the direct results of both types of ablators on separation should be approximately the same (excluding gas-chemistry effects).

Two pressure distributions for the 50-50 phenolic-nylon ablating leading edges are shown in figure 10. These are compared with two graphite-leading-edge pressure distributions at very nearly the same tunnel conditions. With a 30° flap, the pressure distribution for a phenolic-nylon leading edge compares favorably with that for a graphite leading edge. This agreement indicates little or no effect due to mass addition on either plateau pressure or extent of separation and is in line with the results of Kuehn (ref. 2). A comparison of the pressure distributions for the 35° flap, on the other hand, indicates a slight increase in both the plateau pressure and the extent of separation. The primary difference appears to be due to slight leading-edge regression rather than due to mass addition or ablation chemistry. This result can be graphically illustrated with the pressure distributions from a typical teflon ablation test. Figure 11 shows the pressure distributions from a teflon-leading-edge test compared with the pressure distribution from a graphite-leading-edge test at approximately the same tunnel conditions. The three teflon pressure distributions shown were obtained from the same test at different time intervals. The pressure-sensing system was subjected to an overpressure during tunnel starting conditions to prevent the blowing of any foreign particles into the sensors. Therefore, the time dependence shown in figure 11 is not due to a pressure lag since the curves would appear in reverse order if this were true. On the other hand, these are fairly regular intervals and correspond almost directly to the leading-edge-regression values given in the tabular key at the top of the figure. In other words, the increases in extent of separation appear to be directly proportional to the amount of leading-edge regression that has occurred. It appears, then, that there is negligible direct effect of mass addition on separation whereas the indirect effect of leading-edge regression can have significant effect on both the extent and plateau-pressure level, at least for this geometry and under the conditions of these tests.

When the plateau pressures from the ablation tests were compared with equation (1), approximately the same deviation as in previous tests was encountered. (See solid circular symbols in fig. 7.) There appears to be a definite change in plateau-pressure level

between these data and those obtained on a similar nonablative model in reference 3. However, as can be seen in figure 11, separation on the teflon-leading-edge model became so extensive that a definite experimental pressure gradient at the interaction point could not be determined. The assumed pressure gradient required to calculate local flow properties could easily be in enough error to account for the differences shown in figure 7.

Calculations for the extent of separation by the method of reference 3 were compared with the ablation data and are presented in figure 12. The three curves shown represent three different velocity profiles initially assumed. Reference 3 previously established the exponential profile as the one giving the best results at conditions similar to the present tests. The additional profiles are shown only to illustrate the amount of change in results which can be obtained by assuming various velocity profiles. The agreement is good for teflon ablation at the early time intervals and becomes progressively worse with time. Significant leading-edge regression has occurred even at the earliest time that data could be obtained. If the trend were extrapolated back to zero time, the agreement for the teflon results would be expected to be about the same as that shown for phenolic nylon. Thus, a general trend toward overprediction of extent of separation existed throughout this study. That this method tended to overpredict the extent of separation slightly had been previously implied in figure 9. However, the disagreement shown in figure 12 is considered small, and the technique gives reasonable results in regions of strong interaction.

CONCLUDING REMARKS

An investigation has been made of real-gas laminar-boundary-layer separation in low-density air. A series of tests were undertaken to establish the validity of certain perfect-gas relations for separation plateau pressure and to measure the extent of separation at low-density conditions. Limited studies of the effect of leading-edge bluntness and ablation on the extent of separation were also made. The results of the investigation indicate the following:

(1) The simple relation for laminar plateau-pressure coefficient used as a basis for comparison maintains approximately the same accuracy for the conditions of this study as for previous experimental data. However, the overall accuracy of this simple relation over a broad Mach number and Reynolds number range does not appear to be adequate to allow indiscriminate use for all laminar separation and a more comprehensive study of this problem should be undertaken.

(2) Increasing low-density effects not predicted by strong-interaction theory were found to delay the onset of separation.

(3) Increasing leading-edge bluntness was found to increase the apparent extent of separation at the conditions of the present tests. This increase in the extent of separation is believed to be a result of the presence of rarefaction effects for small leading-edge bluntnesses.

(4) The direct effect of mass addition, through 50-50 phenolic-nylon and teflon ablative leading edges, on the extent of separation was found to be negligible. However, an indirect effect of leading-edge regression because of ablation was found to have a significant effect on the extent of separation and plateau-pressure levels.

Langley Research Center,
National Aeronautics and Space Administration,
Langley Station, Hampton, Va., June 24, 1968,
129-01-03-15-23.

REFERENCES

1. Kuehn, Donald M.: Laminar Boundary-Layer Separation Induced by Flares on Cylinders With Highly Cooled Boundary Layers at a Mach Number of 15. NASA TN D-2610, 1965.

2. Kuehn, D. M.; and Monson, D. J.: Boundary-Layer Separation and Reattachment With and Without Ablation. Separated Flows, Pt. I, AGARD CP No. 4, May 1966, pp. 121-145.

3. Anders, John B.; and Edwards, C. L. W.: A Real-Gas Study of Low-Density Wedge-Induced Laminar Separation on a Highly Cooled Blunt Flat Plate at $M_\infty = 12$. NASA TN D-4320, 1968.

4. Schlichting, Hermann (J. Kestin, trans.): Boundary Layer Theory. McGraw-Hill Book Co., Inc., 1955, pp. 297-307.

5. Thwaites, B.: Approximate Calculation of the Laminar Boundary Layer. Aeronaut. Quart., vol. I, pt. III, Nov. 1949, pp. 245-280.

6. Makofski, R. A.: A Two-Parameter Method for Shock Wave-Laminar Boundary Layer Interaction and Flow Separation. Proceedings of the 1963 Heat Transfer and Fluid Mechanics Institute, Anatol Roshko, Bradford Sturtevant, and D. R. Bartz, editors, Stanford Univ. Press, c.1963, pp. 112-127.

7. Crocco, Luigi; and Lees, Lester: A Mixing Theory for the Interaction Between Dissipative Flows and Nearly Isentropic Streams. J. Aeronaut. Sci., vol. 19, no. 10, Oct. 1952, pp. 649-676.

8. Glick, Herbert S.: Modified Crocco-Lees Mixing Theory for Supersonic Separated and Reattaching Flows. J. Aerospace Sci., vol. 29, no. 10, Oct. 1962, pp. 1238-1249.

9. Tani, Itiro: On the Approximate Solution of the Laminar Boundary-Layer Equations. J. Aeronaut. Sci., vol. 21, no. 7, July 1954, pp. 487-495, 504.

10. Lees, Lester; and Reeves, Barry L.: Supersonic Separated and Reattaching Laminar Flows: I. General Theory and Application to Adiabatic Boundary-Layer/Shock-Wave Interactions. AIAA J., vol. 2, no. 11, Nov. 1964, pp. 1907-1920.

11. Chapman, Dean R.; Kuehn, Donald M.; and Larson, Howard K.: Investigation of Separated Flows in Supersonic Streams With Emphasis on the Effect of Transition. NACA Rep. 1356, 1958. (Supersedes NACA TN 3869.)

12. Denison, M. Richard; and Baum, Eric: Compressible Free Shear Layer With Finite Initial Thickness. AIAA J., vol. 1, no. 2, Feb. 1963, pp. 342-349.

13. Kubota, Toshi; and Dewey, C. Forbes, Jr.: Momentum Integral Methods for the Laminar Free Shear Layer. AIAA J., vol. 2, no. 4, Apr. 1964, pp. 625-629.

14. Gadd, G. E.: A Simple Theory for Interactions Between Shock Waves and Entirely Laminar Boundary Layers. J. Aeronaut. Sci., vol. 23, no. 3, Mar. 1956, pp. 225-230.

15. Gadd, G. E.: A Theoretical Investigation of Laminar Separation in Supersonic Flow. J. Aeronaut. Sci., vol. 24, no. 10, Oct. 1957, pp. 759-771, 784.

16. Gadd, G. E.: Boundary Layer Separation in the Presence of Heat Transfer. AGARD Rep. 280, Apr. 1960.

17. Nielsen, J. N.; Lynes, L. L.; Goodwin, F. K.; and Holt, M.: Calculation of Laminar Separation With Free Interaction by the Method of Integral Relations. AIAA Paper No. 65-50, Jan. 1965.

18. Boatright, W. B.; Stewart, R. B.; and Sebacher, D. I.: Testing Experience and Calibration Experiments in a Mach Number 12, 1-Foot Hypersonic Arc Tunnel. Third Hypervelocity Techniques Symposium, Univ. of Denver and Arnold Eng. Develop. Center, Mar. 1964, pp. 182-212.

19. Stewart, Roger B.: A Calorimeter Study of a Magnetically Stabilized Arc-Heater. AIAA J., vol. 2, no. 2, Feb. 1964, pp. 384-386.

20. Duckett, Roy J.; and Sebacher, Daniel I.: Velocity Measurements in the Langley 1-Foot (0.305-Meter) Hypersonic Arc Tunnel. NASA TN D-3308, 1966.

21. Guy, R. W.; and Winebarger, R. M.: Effect of Orifice Size and Heat-Transfer Rate on Measured Static Pressures in a Low-Density, Arc-Heated Wind Tunnel. NASA TN D-3829, 1967.

22. Hakkinen, R. J.; Greber, I.; Trilling, L.; and Abarbanel, S. S.: The Interaction of an Oblique Shock Wave With a Laminar Boundary Layer. NASA MEMO 2-18-59W, 1959.

23. Sterrett, James R.; and Emery, James C.: Extension of Boundary-Layer-Separation Criteria to a Mach Number of 6.5 by Utilizing Flat Plates With Forward-Facing Steps. NASA TN D-618, 1960.

24. Curle, N.: The Laminar Boundary Layer Equations. Clarendon Press (Oxford), 1962.

25. McCroskey, William J.: An Experimental Model for the Sharp Leading Edge Problem in Rarefied Hypersonic Flow. ARL 66-0101, U.S. Air Force, June 1966. (Available from DDC as AD 641996.)

26. Talbot, L.: Criterion for Slip Near the Leading Edge of a Flat Plate in Hypersonic Flow. AIAA J. (Tech. Notes and Comments), vol. 1, no. 5, May 1963, pp. 1169-1171.

27. Townsend, James C.: Effects of Leading-Edge Bluntness and Ramp Deflection Angle on Laminar Boundary-Layer Separation in Hypersonic Flow. NASA TN D-3290, 1966.

28. Kuehn, Donald M.: Blast-Wave Correlation of Pressures on Blunt-Nosed Cylinders in Perfect- and Real-Gas Flows at Hypersonic Speeds. AIAA J., vol. 1, no. 3, Mar. 1963, pp. 716-717.

29. Harris, Julius E.: Aerodynamic Characteristics of a Series of Spherically Blunted 10^{o} Cones With 30^{o} and 60^{o} Base Flares. NASA TN D-3675, 1966.

30. Vas, I. E.; McDougall, J.; Koppenwallner, G.; and Bogdonoff, S. M.: Some Exploratory Experimental Studies of Hypersonic Low Density Effects on Flat Plates and Cones. Rarefied Gas Dyn., Vol. I. J. H. deLeeuw, ed., Academic Press, 1965, pp. 508-534.

31. Nagamatsu, H. T.; Sheer, R. E., Jr.; and Schmid, J. R.: High Temperature Rarefied Hypersonic Flow Over a Flat Plate. ARS J., vol. 31, no. 7, July 1961, pp. 902-910.

32. Vidal, R. J.; and Wittliff, C. E.: Hypersonic Low Density Studies of Blunt and Slender Bodies. Rarefied Gas Dyn., Vol. II, J. A. Laurmann, ed., Academic Press, 1963, pp. 343-378.

33. Deskins, H. Eugene: Correlation of Flat-Plate Pressures Using the Rarefaction Parameter $M_{\infty}C_{\infty}^{1/2}/Re_{x_{\infty}}^{1/2}$. AIAA J., vol. 2, no. 3, Mar. 1964, pp. 573-574.

34. Becker, Manfred; and Boylan, David E.: Flow Field and Surface Pressure Measurements in the Fully Merged and Transition Flow Regimes on a Cooled Sharp Flat Plate. AEDC-TR-66-111, U.S. Air Force, Sept. 1966. (Available from DDC as AD 638804.)

35. Pan, Y. S.; and Probstein, Ronald F.: Rarefied Flow Transition at a Leading Edge. Publ. No. 64-8 (Contract Nonr-1841(93)), Fluid Mech. Lab., Massachusetts Inst. Technol., Oct. 1964. (Available from DDC as AD 608 431.)

36. Putnam, Lawrence E.: Investigation of Effects of Ramp Span and Deflection Angle on Laminar Boundary-Layer Separation at Mach 10.03. NASA TN D-2833, 1965.

37. Miller, D. S.; Hijman, R.; and Childs, M. E.: Mach 8 to 22 Studies of Flow Separation Due to Deflected Control Surfaces. AIAA J., vol. 2, no. 2, Feb. 1964, pp. 312-321.

38. Johnson, Charles B.: Pressure and Flow-Field Study at Mach Number 8 of Flow Separation on a Flat Plate With Deflected Trailing-Edge Flap. NASA TN D-4308, 1968.

39. Harvey, William D.: Experimental Investigation of Laminar-Flow Separation on a Flat Plate Induced by Deflected Trailing-Edge Flap at Mach 19. NASA TN D-4671, 1968.

40. Bertram, Mitchel H.; and Blackstock, Thomas A.: Some Simple Solutions to the Problem of Predicting Boundary-Layer Self-Induced Pressures. NASA TN D-798, 1961.

TABLE 1.- TEST CONDITIONS

$[RT_{ref} = 33.86$ Btu/lbm (78.7 kJ/kg); $p_{ref} = 1$ atm$]$

Test	$\frac{H_t}{RT_{ref}}$	$\frac{p_t}{p_{ref}}$	R_∞ per ft	R_∞ per m	M_∞	$\frac{p_{t,2}}{p_{ref}}$	θ, deg	Leading-edge condition
1	46.5	26.9	2.0×10^4	6.6×10^4	13.3	0.0109	1.75	Sharp
2	45.4	29.2	2.4	7.9	13.0	.0135	21.0	
3	49.2	22.4	1.7	5.6	12.7	.0110	26.0	
4	72.4	25.1	1.1	3.6	10.8	.0168	31.5	
5	39.0	27.3	2.7	8.9	13.9	.0103	35.3	
6	48.6	24.7	2.2	7.2	12.2	.0145	*0.250 (0.635)	
7	48.6	27.3	2.1	6.9	12.7	.0104	*0.375 (0.953)	
8	42.7	22.6	2.1	6.9	13.1	.0101	*0.500 (1.270)	
9	43.9	22.4	2.5×10^4	8.2×10^4	13.1	0.0099	35.5	Flat-face blunt
10	44.2	21.4	2.4	7.9	12.9	.0108	35.5	
11	50.0	21.3	1.9	6.2	12.5	.0109	35.5	
12	46.1	20.6	2.1×10^4	6.9×10^4	12.7	0.0108	30.0	Phenolic nylon
13	56.3	22.0	1.5	4.9	12.2	.0109	30.0	Teflon
14	46.4	22.1	1.8	5.9	12.8	.0106	30.0	Graphite
15	53.6	21.2	1.5	4.9	12.3	.0111	35.0	Graphite
16	57.2	21.6	1.3	4.3	12.1	.0111	35.0	Phenolic nylon
17	58.7	22.0	1.2	3.9	12.1	.0112	35.0	Graphite

*For tests 6 to 8, forward-facing steps were used; heights are given first in inches and parenthetically in centimeters.

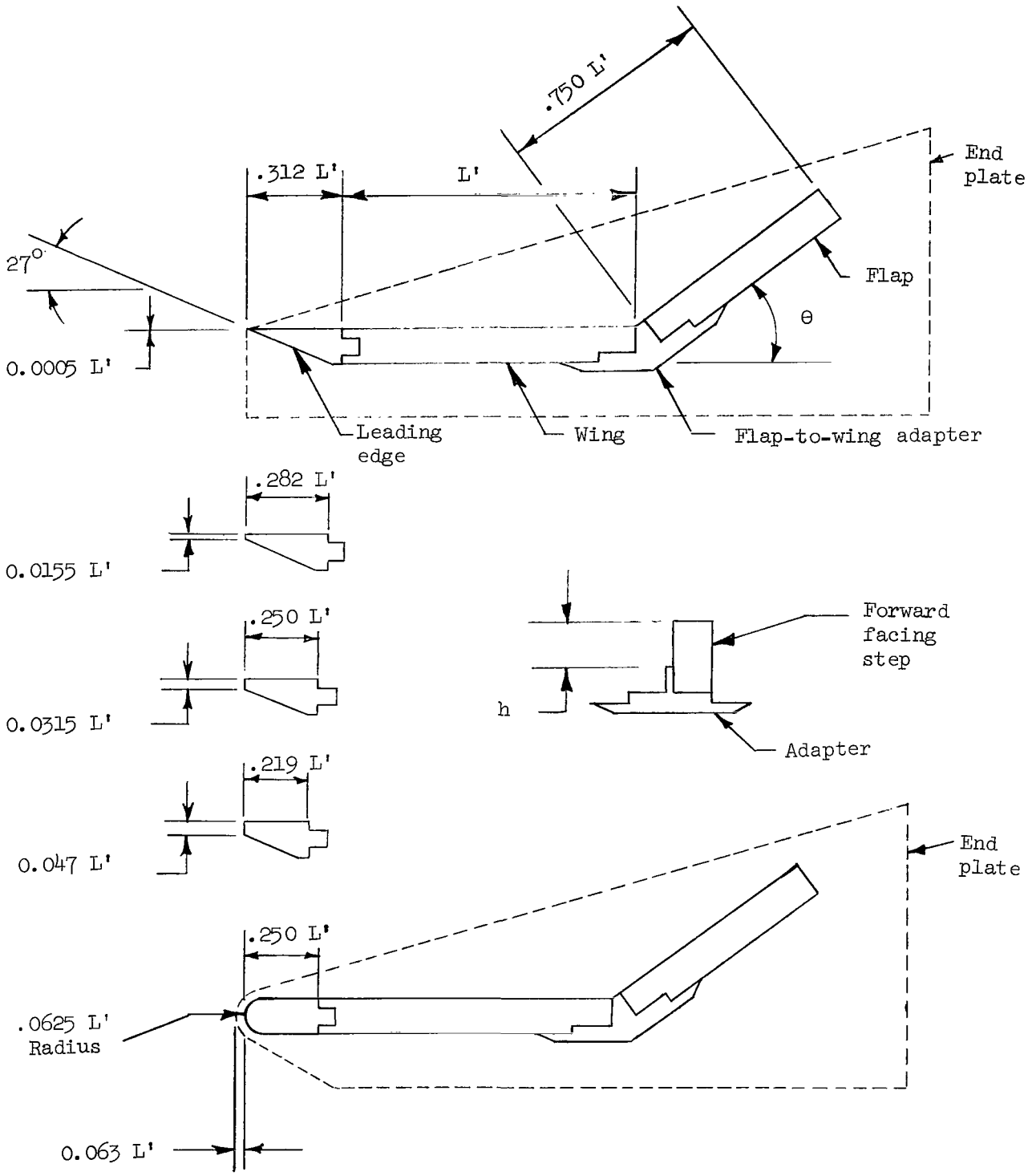

Figure 1.- Schematic drawing of model showing wing, leading edge, and flap. L' = 2.00 in. (5.08 cm).

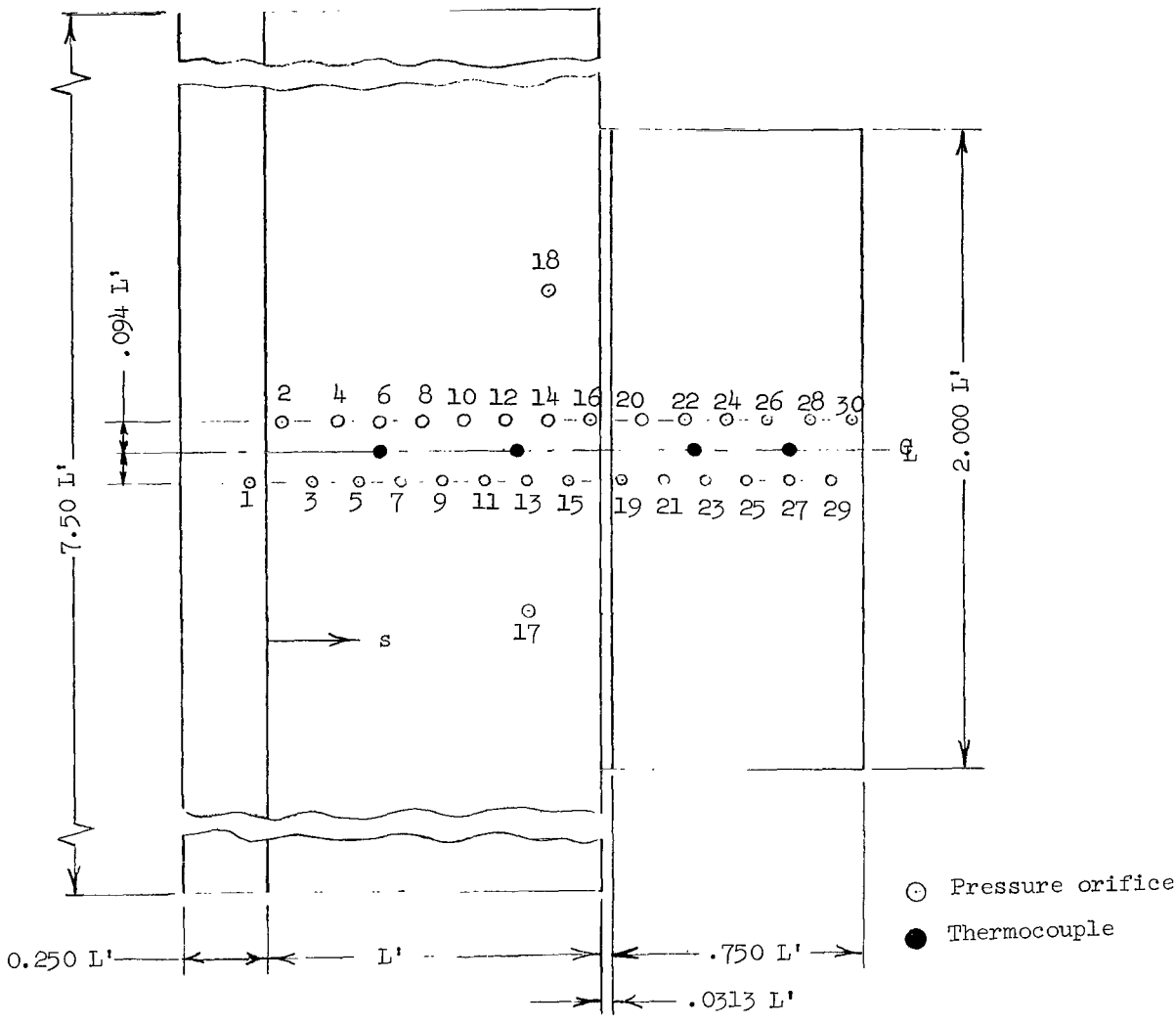

PRESSURE ORIFICES										THERMOCOUPLES	
No.	s/L'	No.	s/L'	No.	s/L'	No.	s/L'	No.	s/L'	No.	s/L'
1	-0.043	7	0.406	13	0.781	19	1.063	25	1.438	1	0.344
2	.051	8	.469	14	.844	20	1.126	26	1.501	2	.750
3	.140	9	.532	15	.906	21	1.188	27	1.563	3	1.282
4	.219	10	.584	16	.969	22	1.251	28	1.626	4	1.594
5	.281	11	.656	17	.781	23	1.313	29	1.688		
6	.344	12	.719	18	.844	24	1.376	30	1.750		

Figure 2.- Model planform showing pressure orifices and thermocouples. L' = 2.00 in. (5.08 cm).

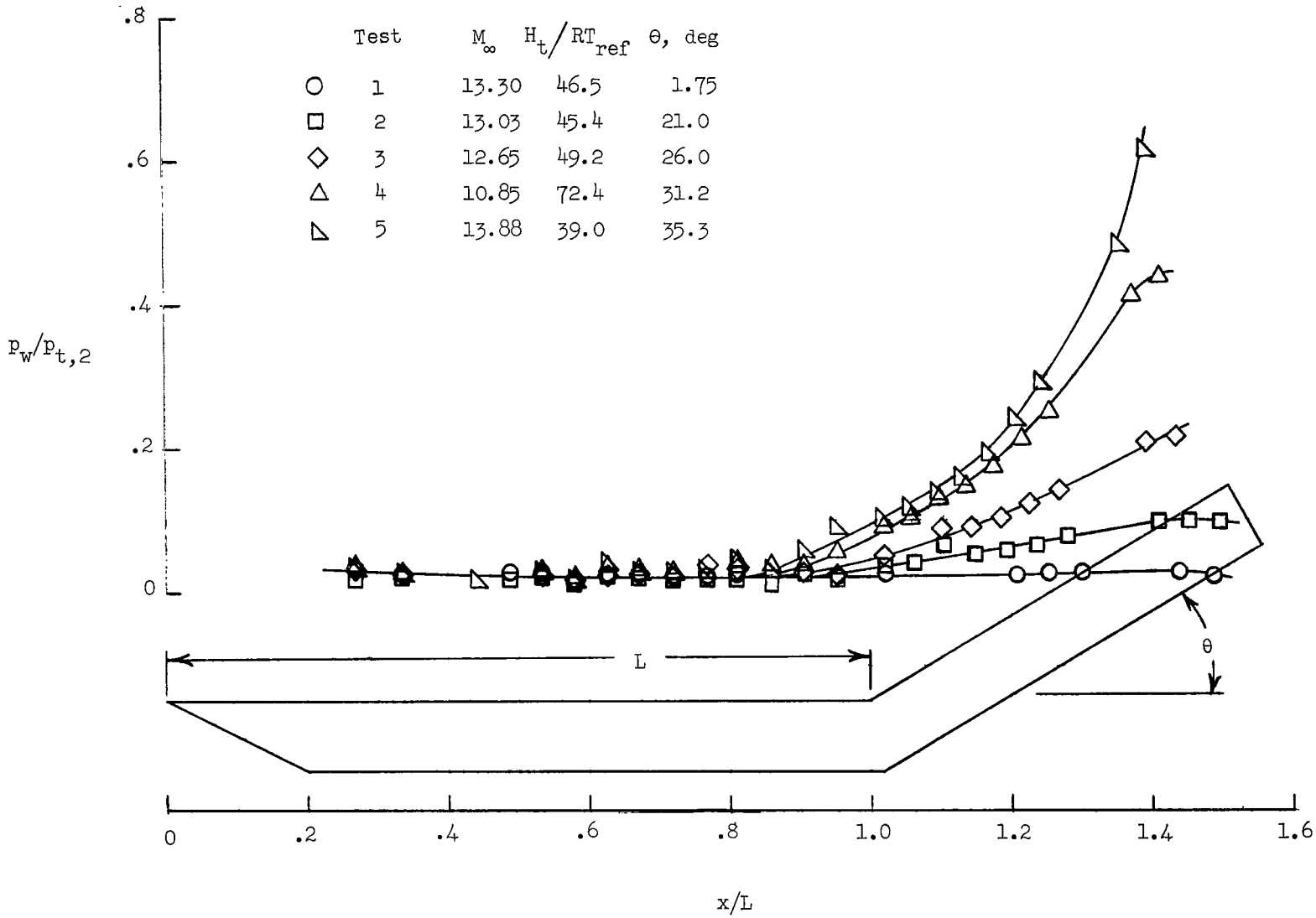

Figure 3.- Typical pressure distribution for cooled sharp plate with flaps. L = 2.625 in. (6.670 cm).

SOURCE		M_∞	R_∞		T_w/T_o
			per in.	per cm	
Vas et al. (ref. 30)	○	26.4	13700	5390	0.150
Nagamatsu et al. (ref. 31)	□	25.1	7350	2890	0.24
Vas et al. (ref. 30)	◇	24.6	6800	2680	0.110
Vidal and Wittliff (ref. 32)	△	22.0	1000	394	0.077
Deskins (ref. 33)	▽	21.4	5800	2280	0.083
Deskins (ref. 33)	▷	21.2	4700	1850	0.083
Vidal and Wittliff (ref. 32)	◁	20.2	520	205	0.082
Deskins (ref. 33)	▷	18.7	8300	3270	0.083
Nagamatsu et al. (ref. 31)	◁	18.5	326	128	~0.08
Vidal and Wittliff (ref. 32)	⌂	14.7	11400	4490	0.100
Becker and Boylan (ref. 34)	◇	10.15	388	153	0.100
Becker and Boylan (ref. 34)	◇	9.19	1700	669	0.200
Present data	◆	12.0	833	328	0.100

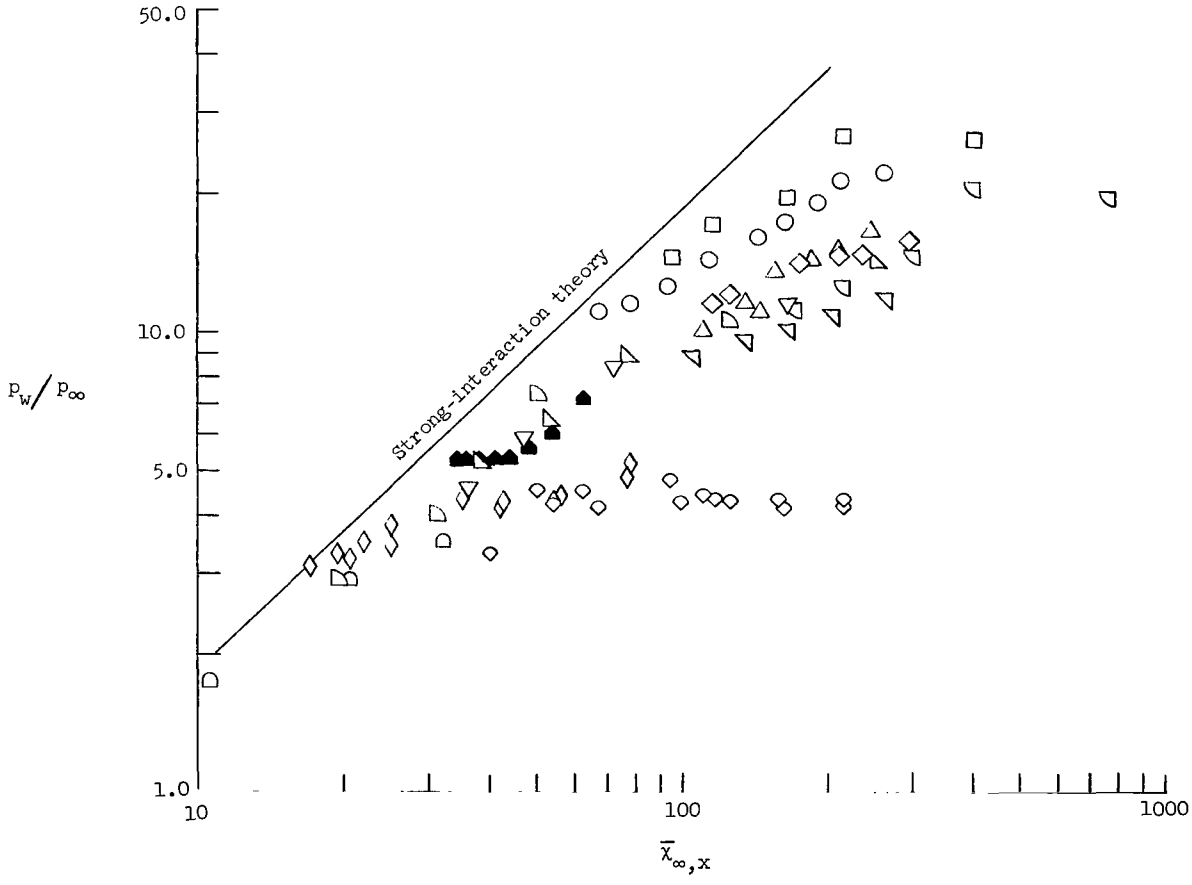

Figure 4.- Available cold-wall sharp-leading-edge flat-plate surface pressures in the merged-layer region.

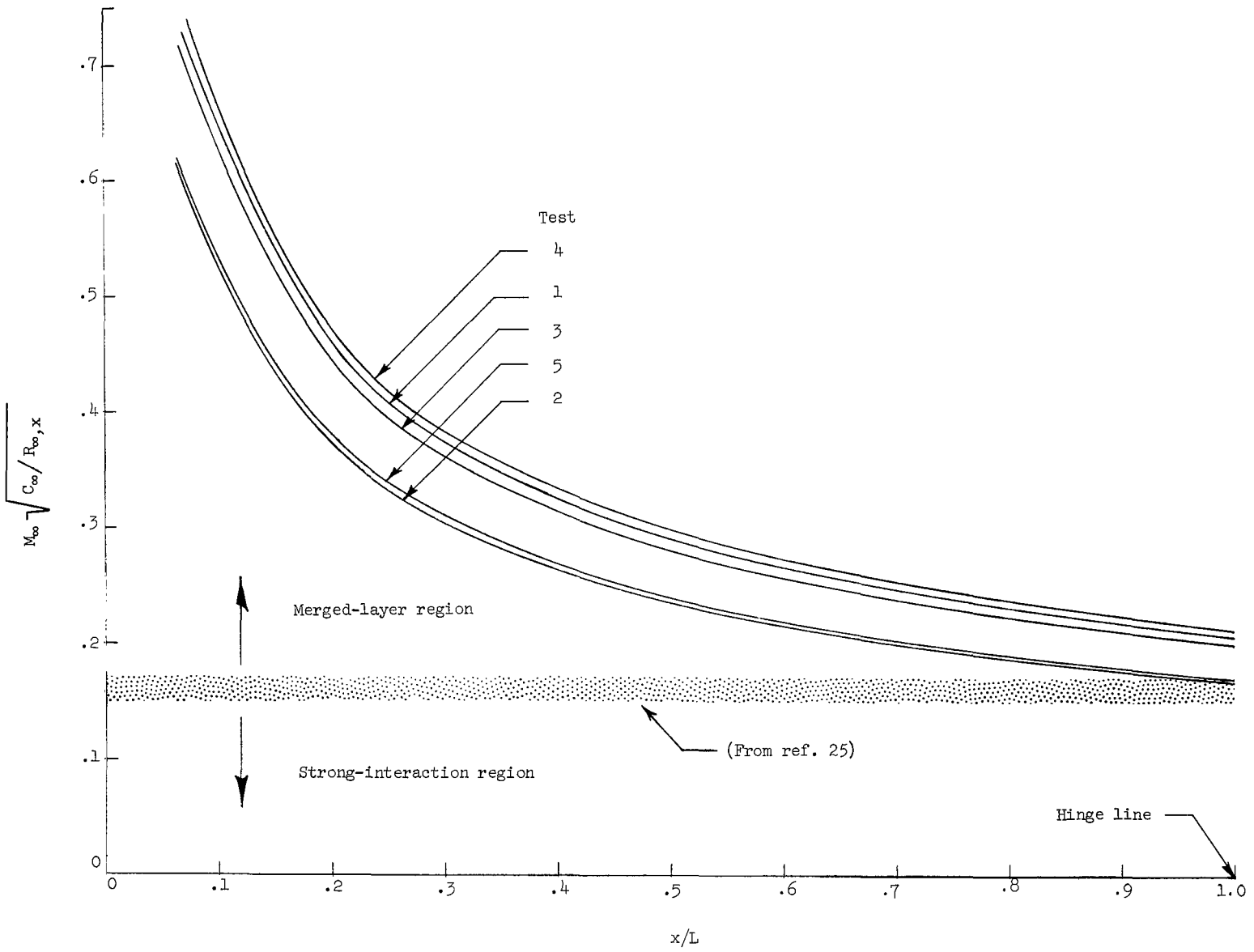

Figure 5.- Variation of rarefaction parameter for sharp-leading-edge flat-plate tests.

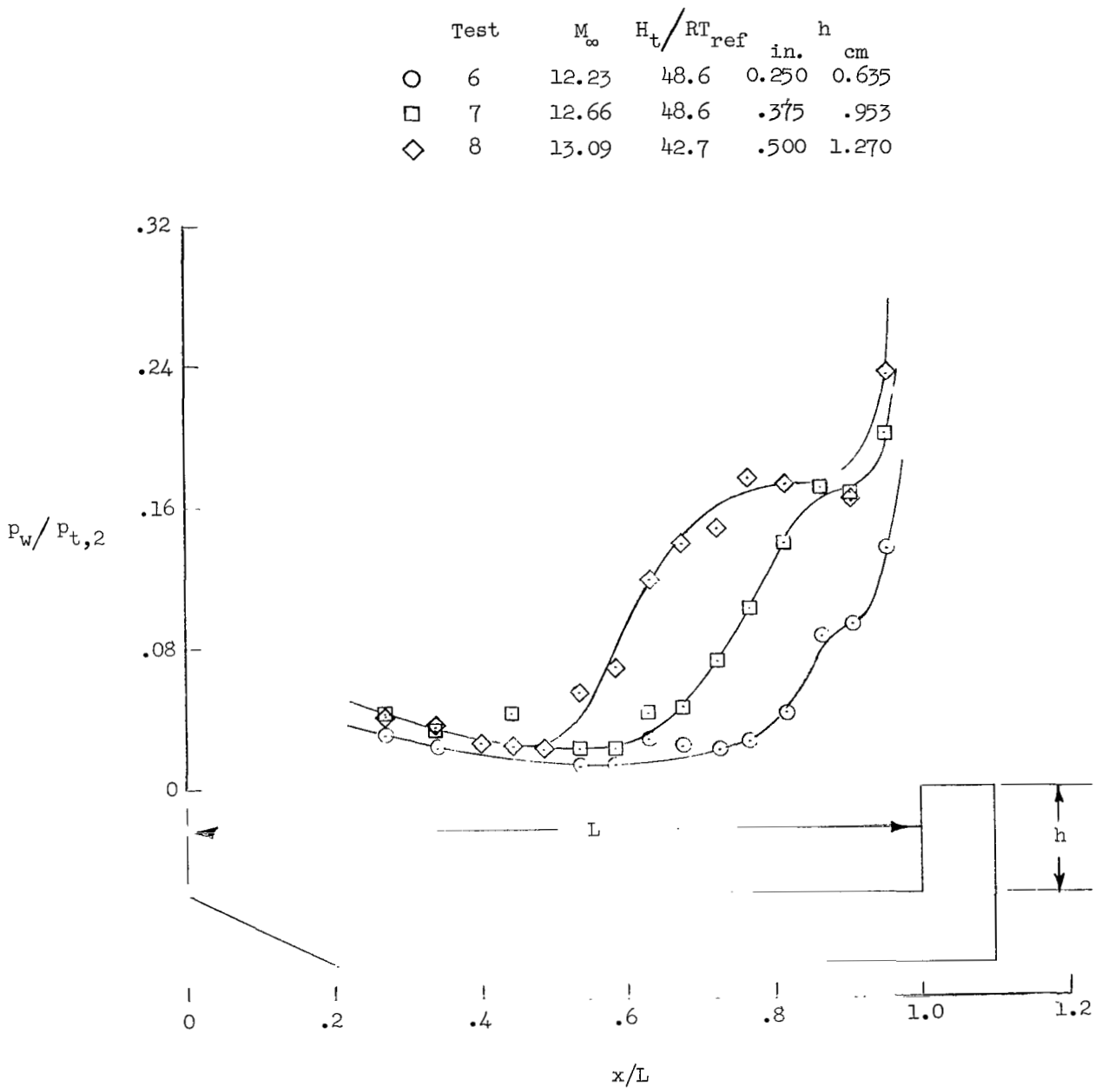

Figure 6.- Typical pressure distribution for cooled sharp plate with uncooled forward-facing steps. L = 2.688 in. (6.82 cm).

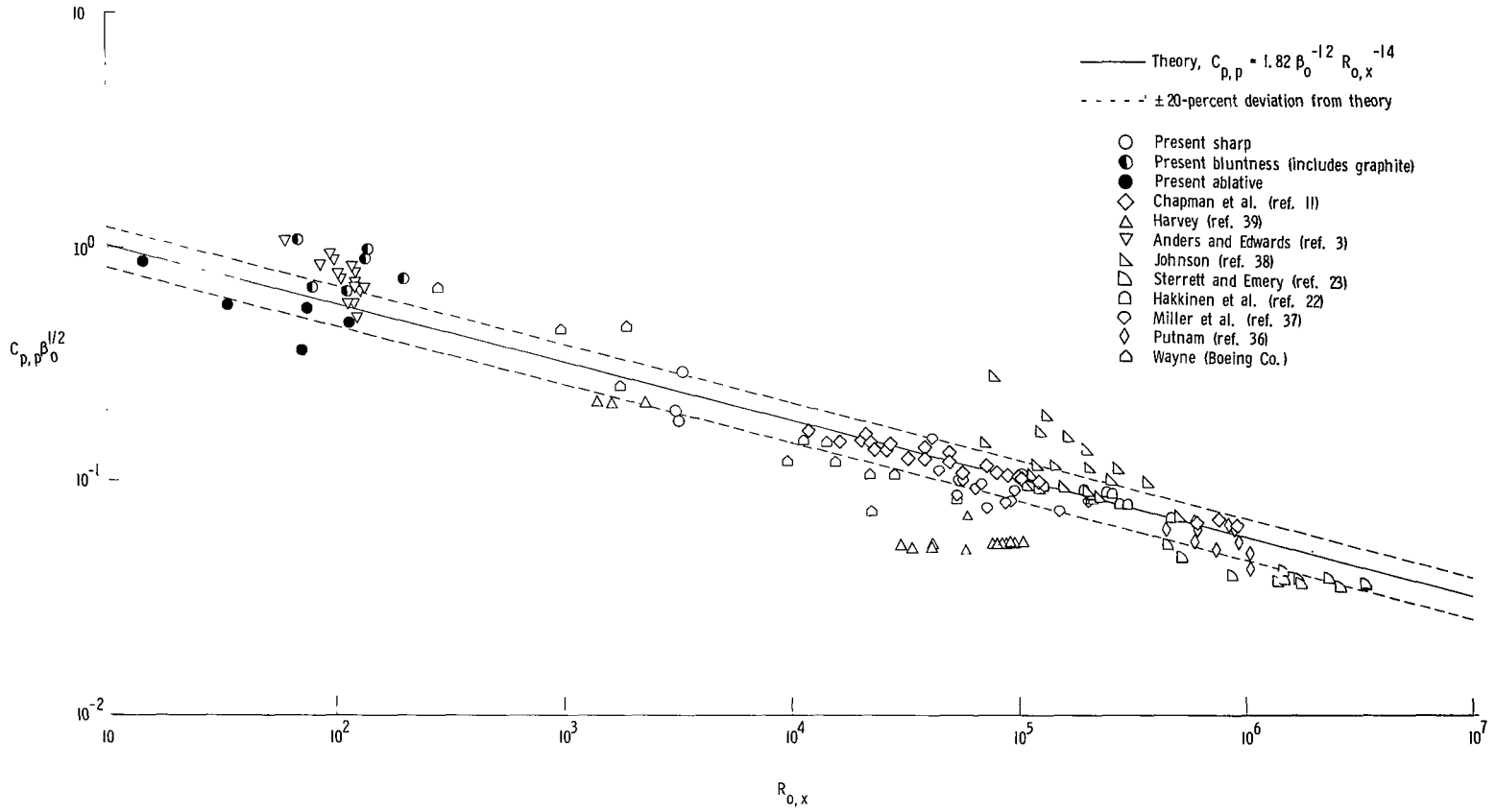

Figure 7.- Plateau-pressure-coefficient correlation.

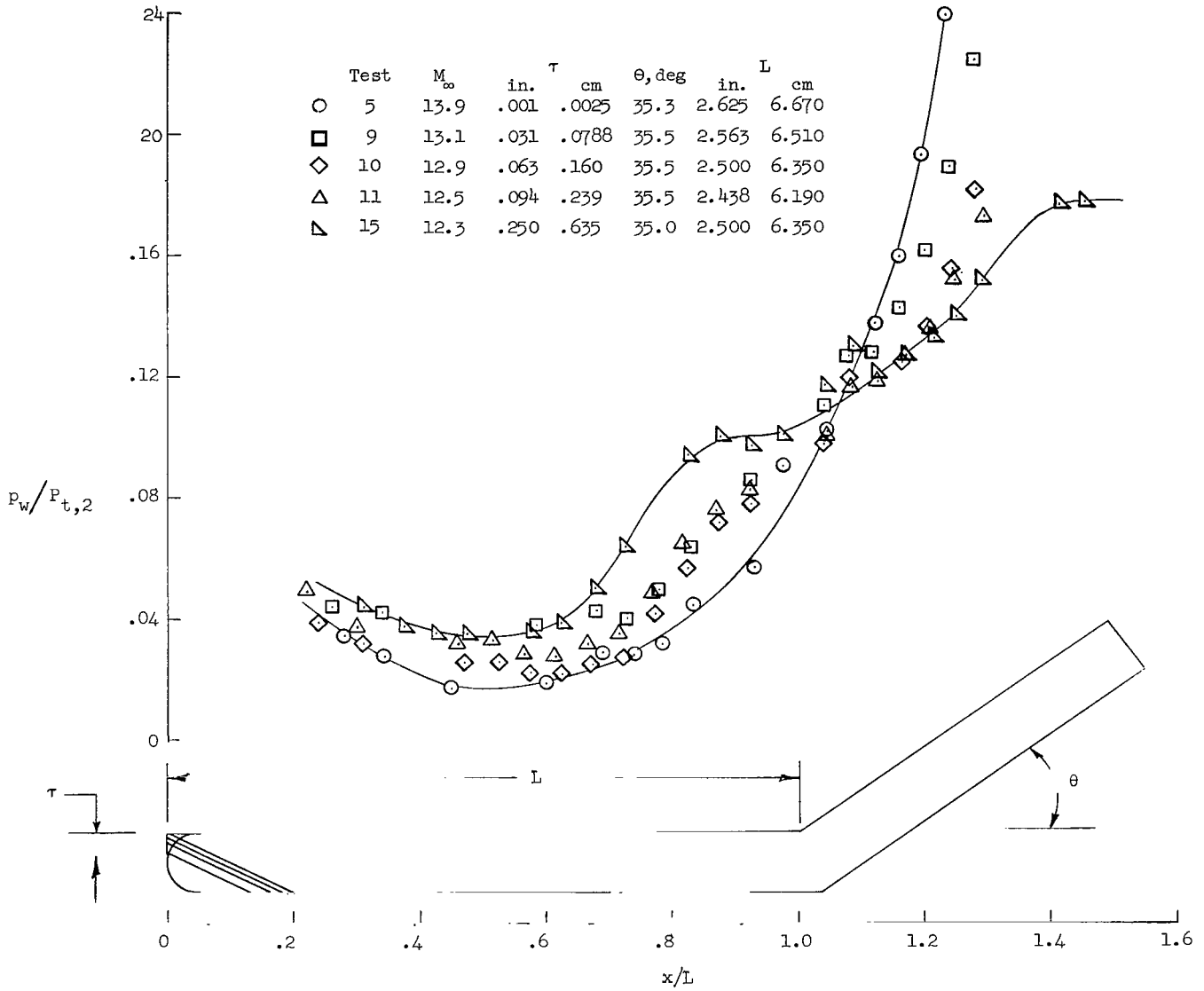

Figure 8.- Typical pressure distributions for leading-edge bluntness effects on extent of separation.

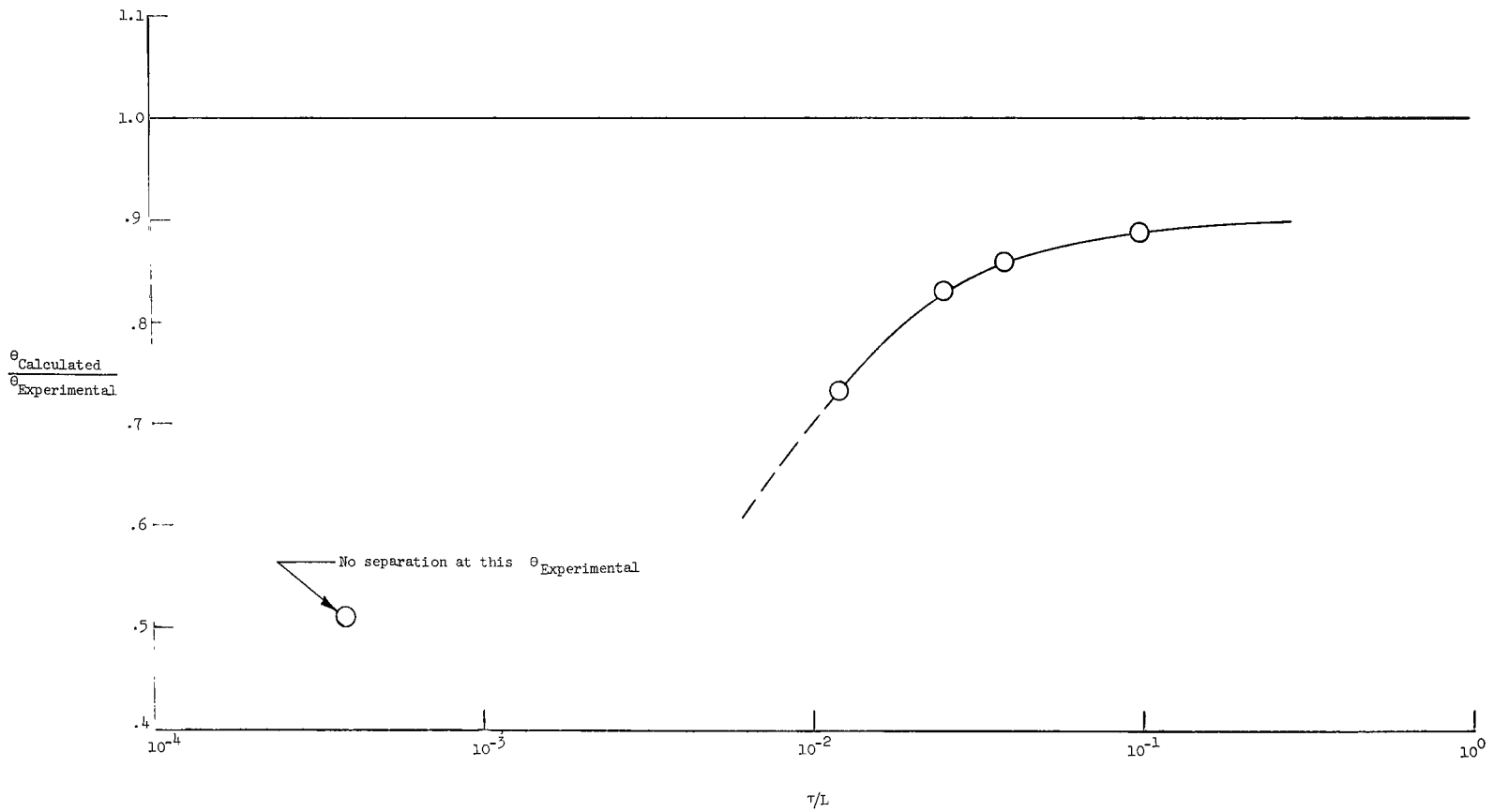

Figure 9.- Nose-bluntness effects on agreement with theory.

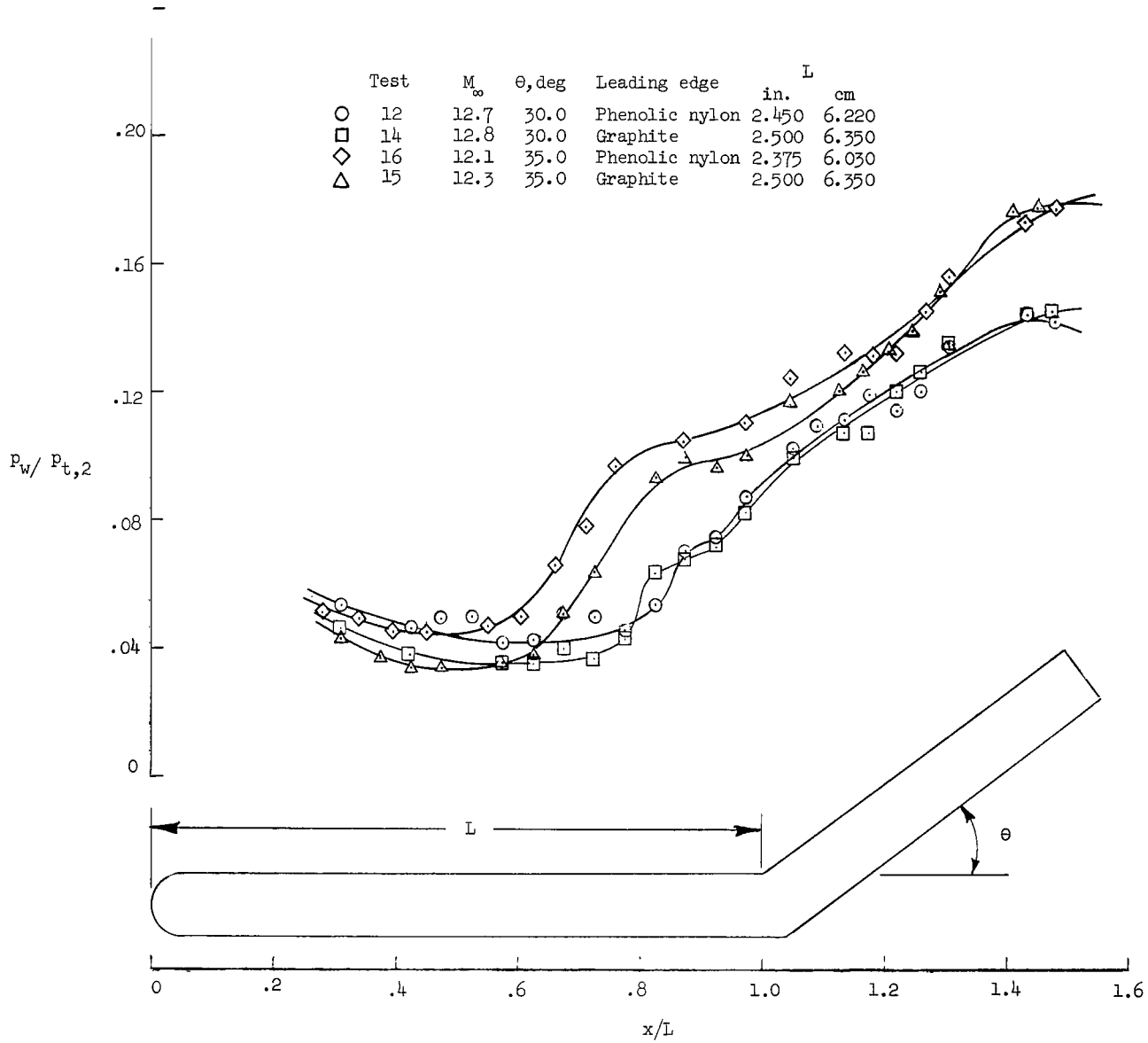

Figure 10.- Typical pressure distributions for phenolic-nylon leading-edge ablation compared with pressure distributions for the nonablative graphite leading edge.

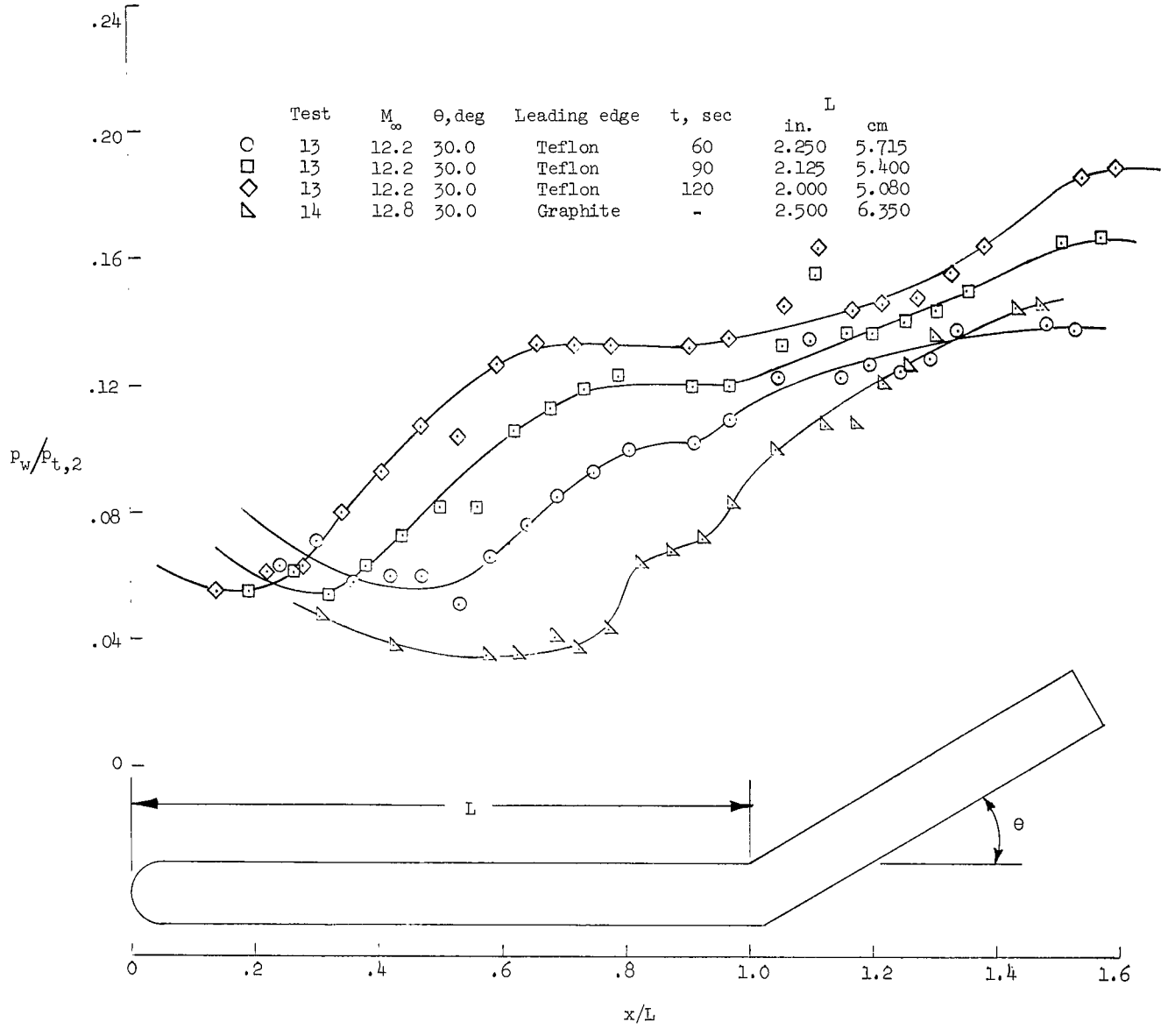

Figure 11.- Typical pressure distributions for teflon leading-edge ablation compared with a pressure distribution for the nonablative graphite leading edge.

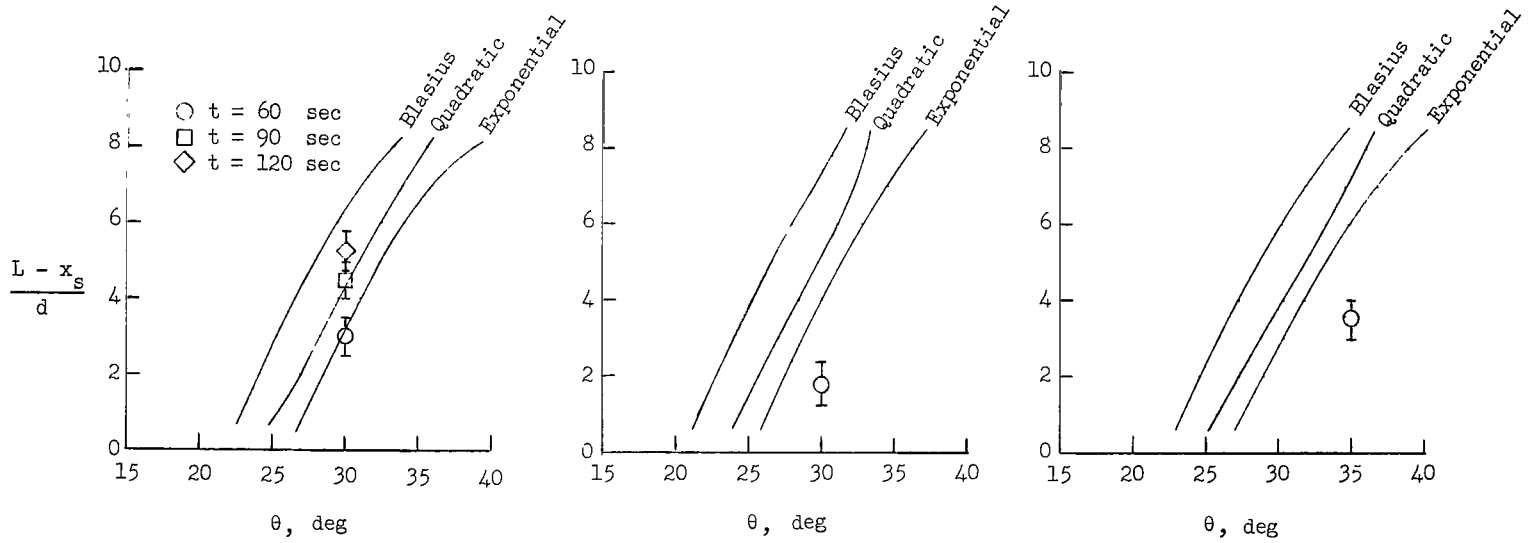

(a) Teflon; $M_\infty = 12.2$; $H_t/RT_{ref} = 56.3$.

(b) Phenolic nylon; $M_\infty = 12.7$; $H_t/RT_{ref} = 46.1$.

(c) Phenolic nylon; $M_\infty = 12.1$; $H_t/RT_{ref} = 57.2$.

Figure 12.- Extent of separation for ablative leading edges compared with theory.

NATIONAL AERONAUTICS AND SPACE ADMINISTRATION
WASHINGTON, D.C. 20546

OFFICIAL BUSINESS

FIRST CLASS MAIL

POSTAGE AND FEES PAID
NATIONAL AERONAUTICS AND
SPACE ADMINISTRATION

"The aeronautical and space activities of the United States shall be conducted so as to contribute . . . to the expansion of human knowledge of phenomena in the atmosphere and space. The Administration shall provide for the widest practicable and appropriate dissemination of information concerning its activities and the results thereof."

—NATIONAL AERONAUTICS AND SPACE ACT OF 1958

NASA SCIENTIFIC AND TECHNICAL PUBLICATIONS

TECHNICAL REPORTS: Scientific and technical information considered important, complete, and a lasting contribution to existing knowledge.

TECHNICAL NOTES: Information less broad in scope but nevertheless of importance as a contribution to existing knowledge.

TECHNICAL MEMORANDUMS: Information receiving limited distribution because of preliminary data, security classification, or other reasons.

CONTRACTOR REPORTS: Scientific and technical information generated under a NASA contract or grant and considered an important contribution to existing knowledge.

TECHNICAL TRANSLATIONS: Information published in a foreign language considered to merit NASA distribution in English.

SPECIAL PUBLICATIONS: Information derived from or of value to NASA activities. Publications include conference proceedings, monographs, data compilations, handbooks, sourcebooks, and special bibliographies.

TECHNOLOGY UTILIZATION PUBLICATIONS: Information on technology used by NASA that may be of particular interest in commercial and other non-aerospace applications. Publications include Tech Briefs, Technology Utilization Reports and Notes, and Technology Surveys.

Details on the availability of these publications may be obtained from:

SCIENTIFIC AND TECHNICAL INFORMATION DIVISION

NATIONAL AERONAUTICS AND SPACE ADMINISTRATION

Washington, D.C. 20546